Supplementary Figure S1

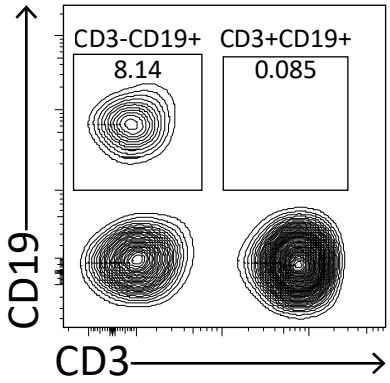

Supplementary Figure S1. Percent CAR T cells in the blood of the patient during therapy (Post-CAR). Flow cytometry shows CD3+CD19+ as a marker of CAR T cells in patient blood during therapy.

Supplementary Figure S2

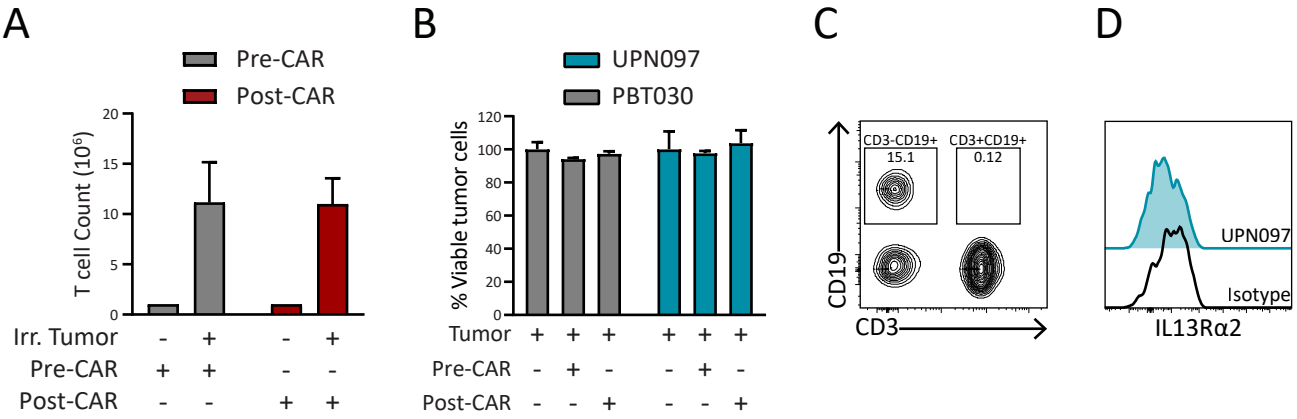

Supplementary Figure S2. Tumor reactivity of endogenous T cell in a non-responder patient. A, T cell count after 14-day co-culture with autologous irradiated (Irr.) patient tumor cell line (UPN097). **B,** In vitro coculture of patient T cells against autologous (UPN097) or nonspecific tumor line (PBT030) at 1:1, E:T ratio. **C,** Flow cytometry shows CD3+CD19+ as a marker of CAR T in patient blood during therapy. **D,** Representative flow cytometry demonstrates IL13Rα2 expression of the patient autologous (UPN097) tumor line. Data are presented as means ± s.e.m.

Supplementary Figure S3

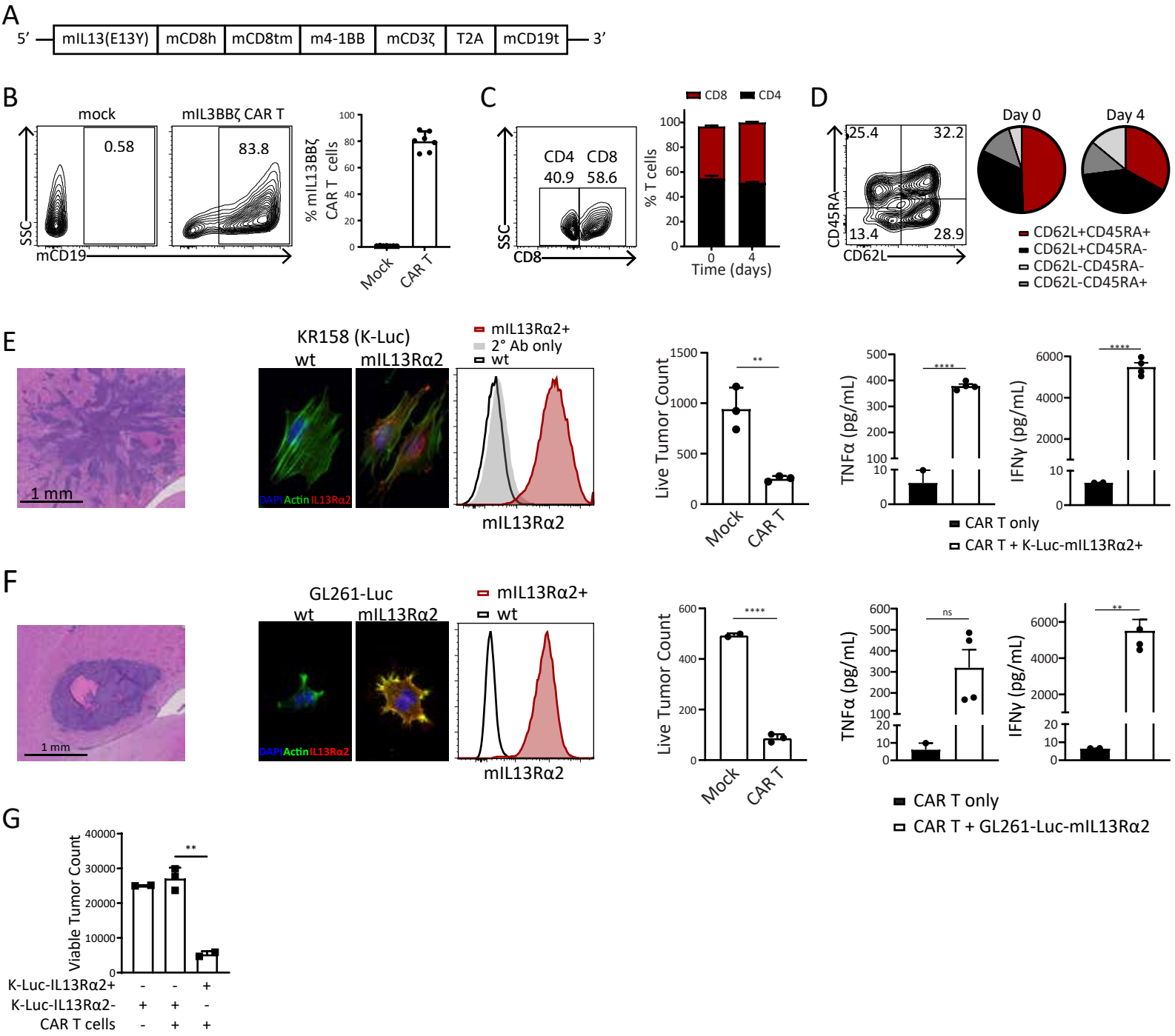

Supplementary Figure S3. mIL13BBζ generation, phenotypic and functional characterization of mIL13BBζ CAR T cells. A, Schematic of the murine IL13Rα2-CAR T (mIL13BBζ CAR T) construct. **B,** Representative flow cytometry (left panel) and graph summarizing percent CAR+ T cells demonstrating transduction efficiency (right panel). **C** and **D,** Flow cytometry and graph depicting phenotypic changes of murine CAR T cell from day 0 to 4. **E,** Representative image of hematoxylin and eosin (H&E) staining shows morphology KR158 tumors. Immunofluorescent and flow cytometry staining confirms transduction of mIL13Rα2 in KR158 (K-Luc) glioma cells (right panel). In vitro killing of mIL13BBζ CAR T cells against K-Luc cells (E:T, 1:3) (middle panel). Luminex ELISA detects TNFα and IFNγ levels after 24 hour coculture of CAR T cells with tumors (E:T, 1:1) (left panel). **F,** Representative image of hematoxylin and eosin (H&E) staining shows morphology of GL261-Luc tumor and immunofluorescent and flow cytometry staining confirms transduction of mIL13Rα2 in GL261-Luc glioma cells (right panel). In vitro killing capacity of mIL13BBζ CAR T cells against IL13Rα2+ GL261-Luc glioma cells (E:T, 1:3) (middle panel) and Luminex ELISA detects TNFα and IFNγ levels 24 hours after coculture (left panel). **G,** In vitro killing of mIL13BBζ CAR T cells against IL13Rα2+ and IL13Rα2- K-Luc cells. Data are representative of at least two independent experiments. Data are presented as means ± s.e.m. and were analyzed by two-tailed, unpaired Student's t-test. *p < 0.05, **p < 0.01, ***p < 0.001 and ****p < 0.0001 for indicated comparison.

Supplementary Figure S4

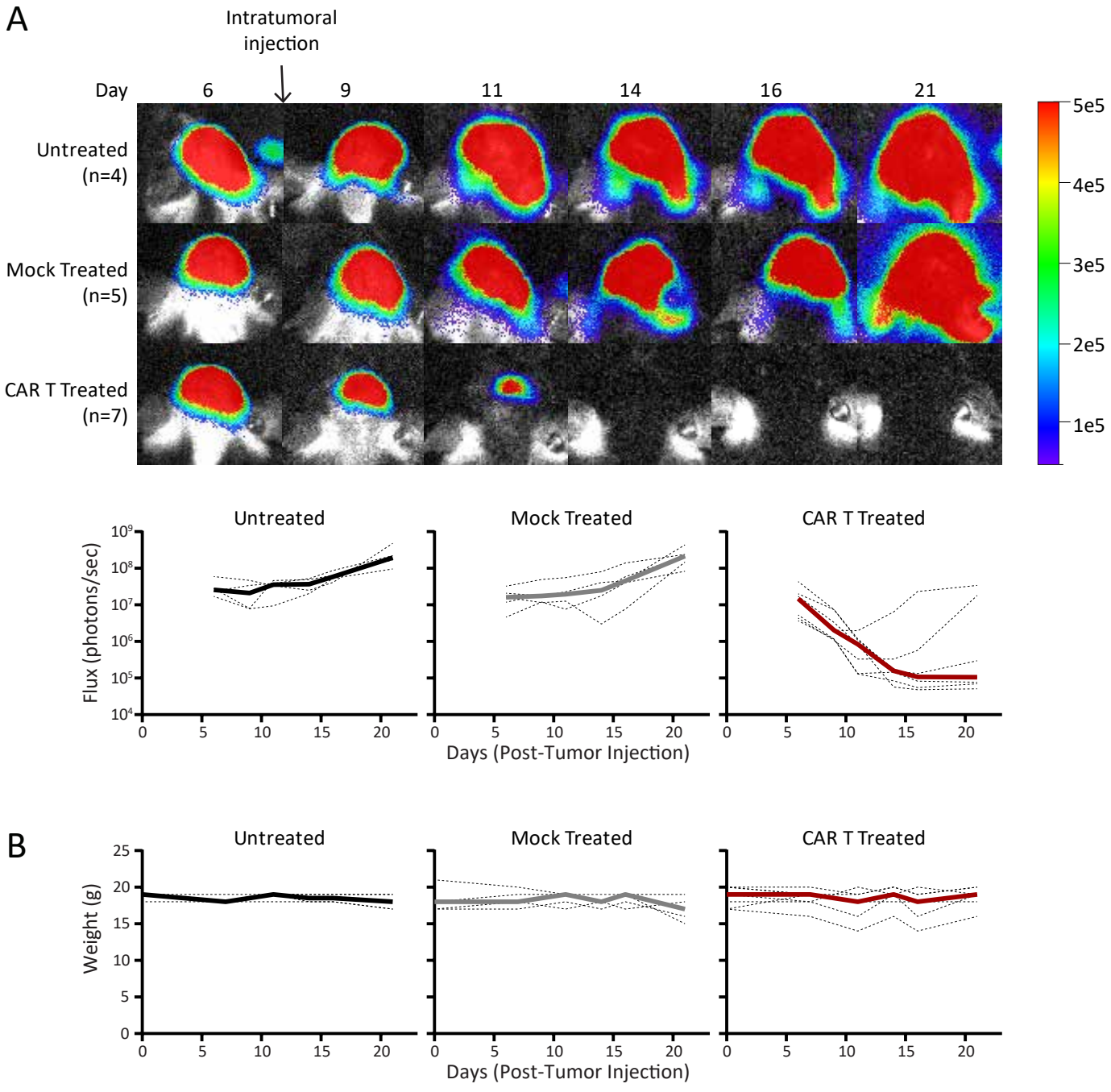

Supplementary Figure S4. mIL13BBζ CAR T cells exhibit potent antitumor activity. A, Representative bioluminescent (BLI) images (top) and flux values (bottom) show tumor growth in untreated (intratumoral injection of PBS), mock treated (intratumoral injection of untransduced T cells) and CAR T treated (intratumoral injection of transduced mIL13BBζ CAR T cells). Individual mice are represented with dotted lines, while median flux is represented by the thick line. **B,** Line graphs show changes in weight in untreated, mock treated and CAR T treated groups. Individual mice are represented with dotted lines, while median weight is represented by the thick line. n=4-7 mice per group.

Supplementary Figure S5

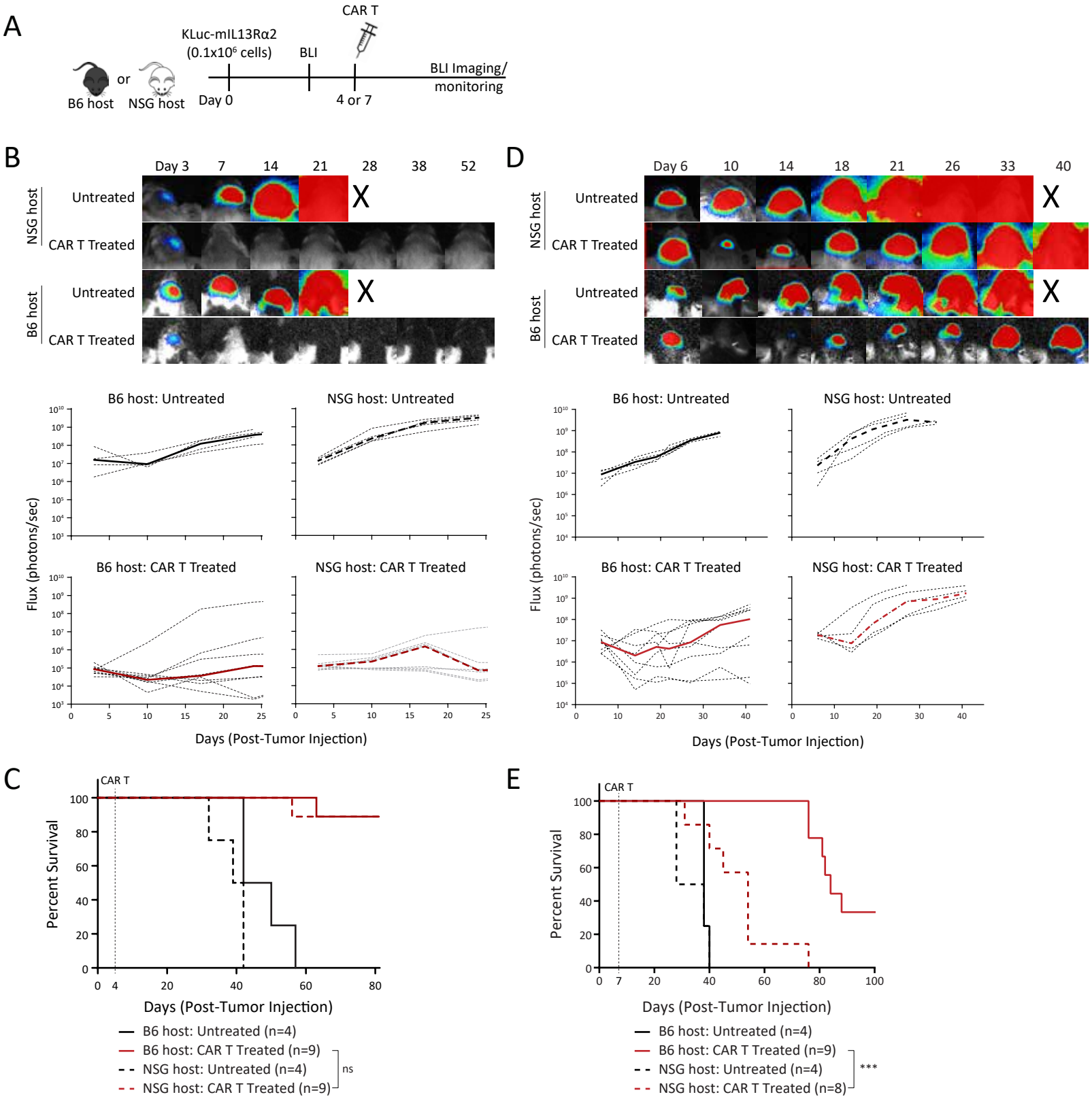

Supplementary Figure S5. mIL13BBζ CAR T cells have superior antitumor activity in immunocompetent host. **A,** Schema of day 4 and 7 in vivo experimental design. **B,** Representative bioluminescent (BLI) images (top) and flux values (bottom) show tumor growth in untreated and CAR T-treated group in 4-day old tumor model. Individual mice are represented with thin dotted lines, while median flux is represented by the thick line. **C,** Survival curve of mice bearing 4-day old K-Luc-mIL13Rα2+ tumors in untreated and CAR T treated groups. **D,** Representative bioluminescent (BLI) images (top) and flux values (bottom) show tumor growth in untreated and CAR T-treated group in 7-day old tumor model Individual mice are represented with thin dotted lines, while median flux is represented by the thick line. **E,** Survival curve of mice bearing 7-day old K-Luc-mIL13Rα2+ tumors in untreated and CAR T-treated groups. Differences between survival curves (**C** and **E**) were analyzed by log-rank (Mantel–Cox) test.

Supplementary Figure S6

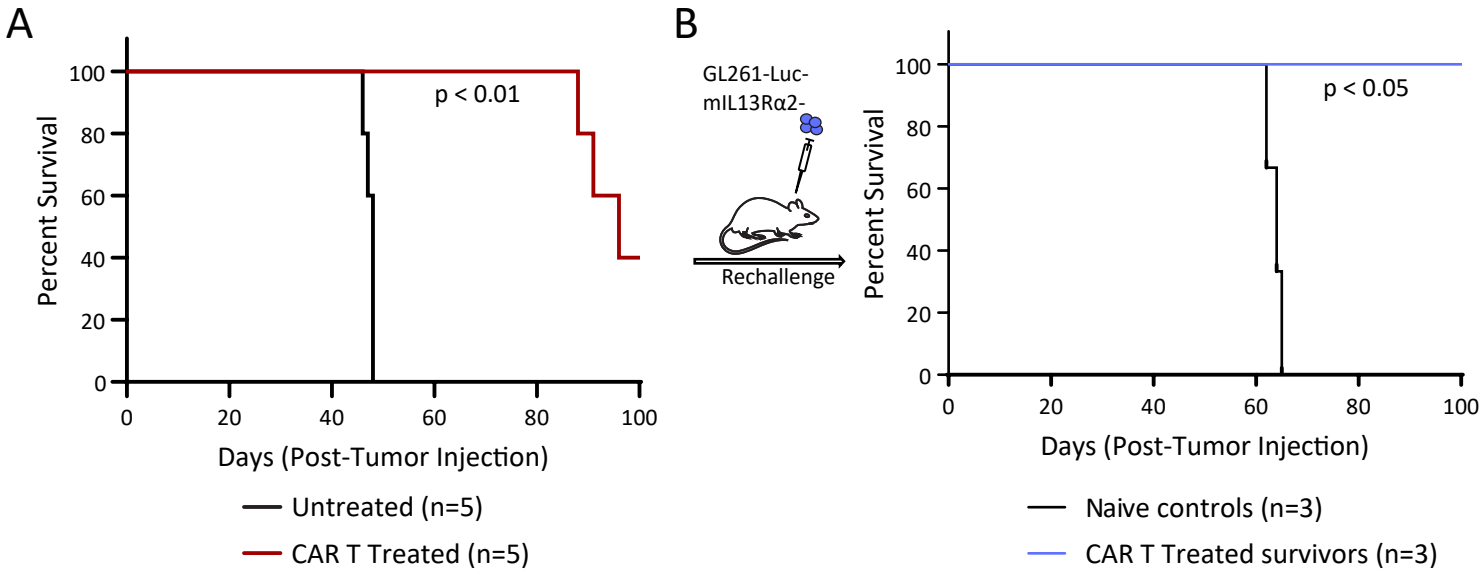

Supplementary Figure S6. mIL13BBζ CAR T cells have potent antitumor activity and induce endogenous memory immune response against GL261-Luc tumors. A, Survival curve of mice bearing mIL13Rα2+ GL261-Luc glioma tumors in untreated and CAR T-treated groups. **B,** Survival of mice cured by the CAR T therapy and rechallenged with IL13Rα2 negative GL261-Luc. Data are representative of at least two independent experiments. *p < 0.05, **p < 0.01, ***p < 0.001 and ****p < 0.0001 for indicated comparison. Differences between survival curves (**A** and **B**) were analyzed by log-rank (Mantel–Cox) test.

Supplementary Figure S7

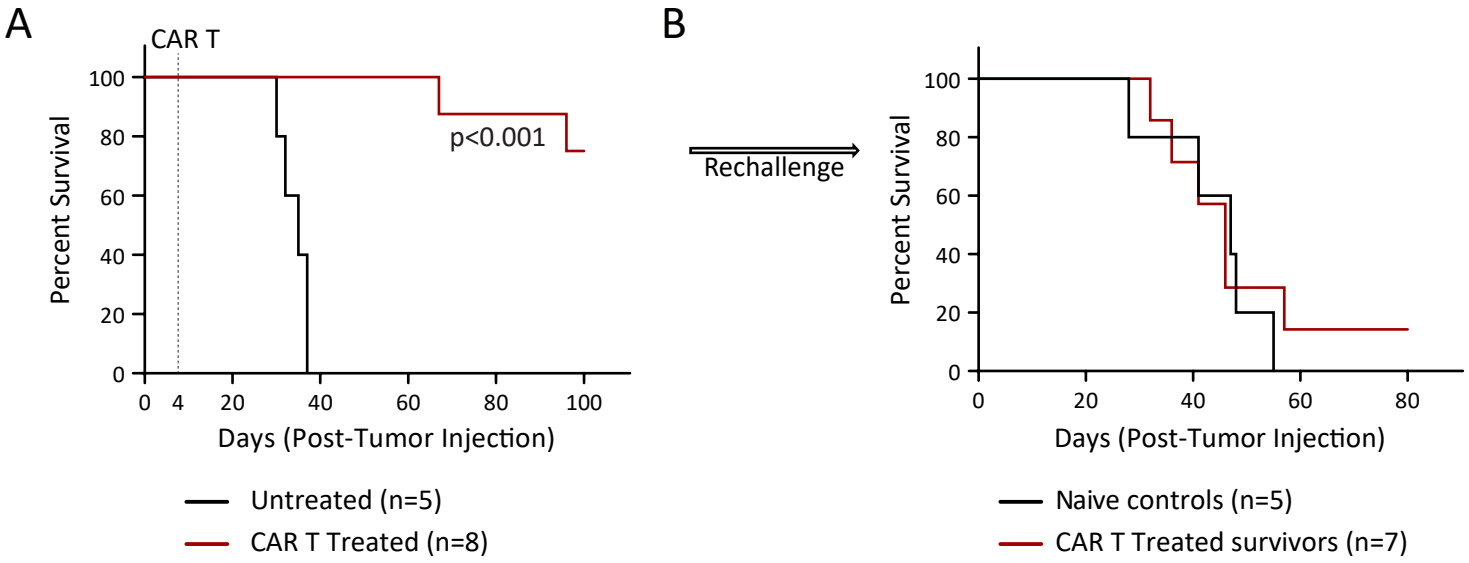

Supplementary Figure S7. mIL13BBζ CAR T cells have potent antitumor activity but are unable to induce endogenous memory immune response in a less established TME. A, Survival curve of mice bearing 4 day-old K-Luc-mIL13Rα2+ tumors in untreated and CAR T treated groups. **B,** Survival of mice cured by the CAR T therapy and rechallenged with IL13Rα2 negative K-Luc tumors. Differences between survival curves (**A**) were analyzed by log-rank (Mantel–Cox) test.

Supplementary Figure S8

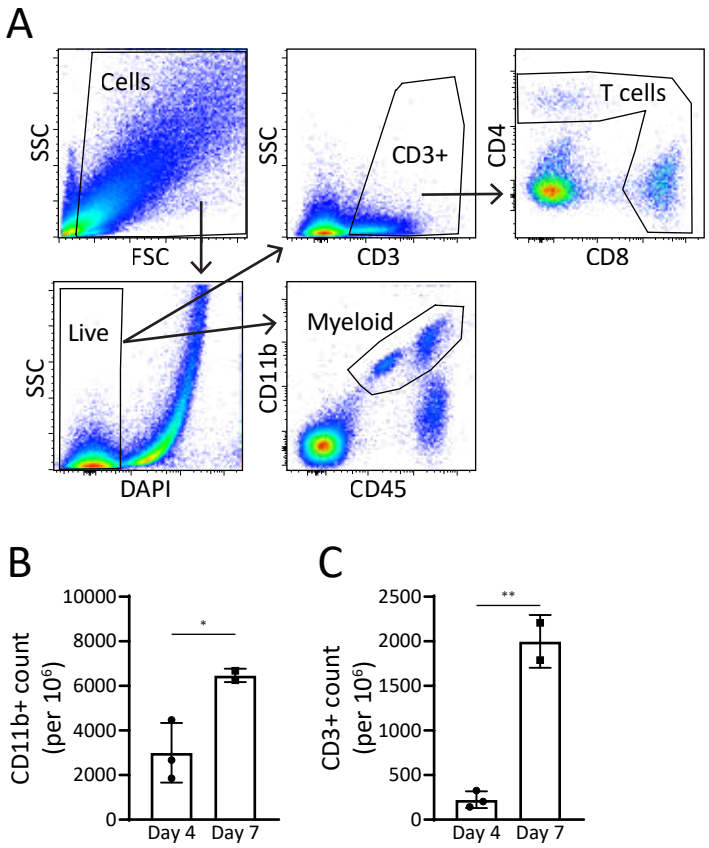

Supplementary Figure S8. Comparison of tumor immune infiltrates in a 4- and 7-day engrafted K-Luc-mIL13Rα2+ tumor. A, Representative flow cytometry and gating strategy of lymphoid and myeloid population in the TME. **B,** Quantification of CD11b and **C,** CD3 cells after flow cytometry sort of untreated, K-Luc-mIL13Rα2+ tumor bearing mice. Each symbol represents one individual. Data are presented as means ± s.e.m. and were analyzed by two-tailed, unpaired Student's t-test. *$p < 0.05$, **$p < 0.01$, ***$p < 0.001$ and ****$p < 0.0001$ for indicated comparison.

Supplementary Figure S9

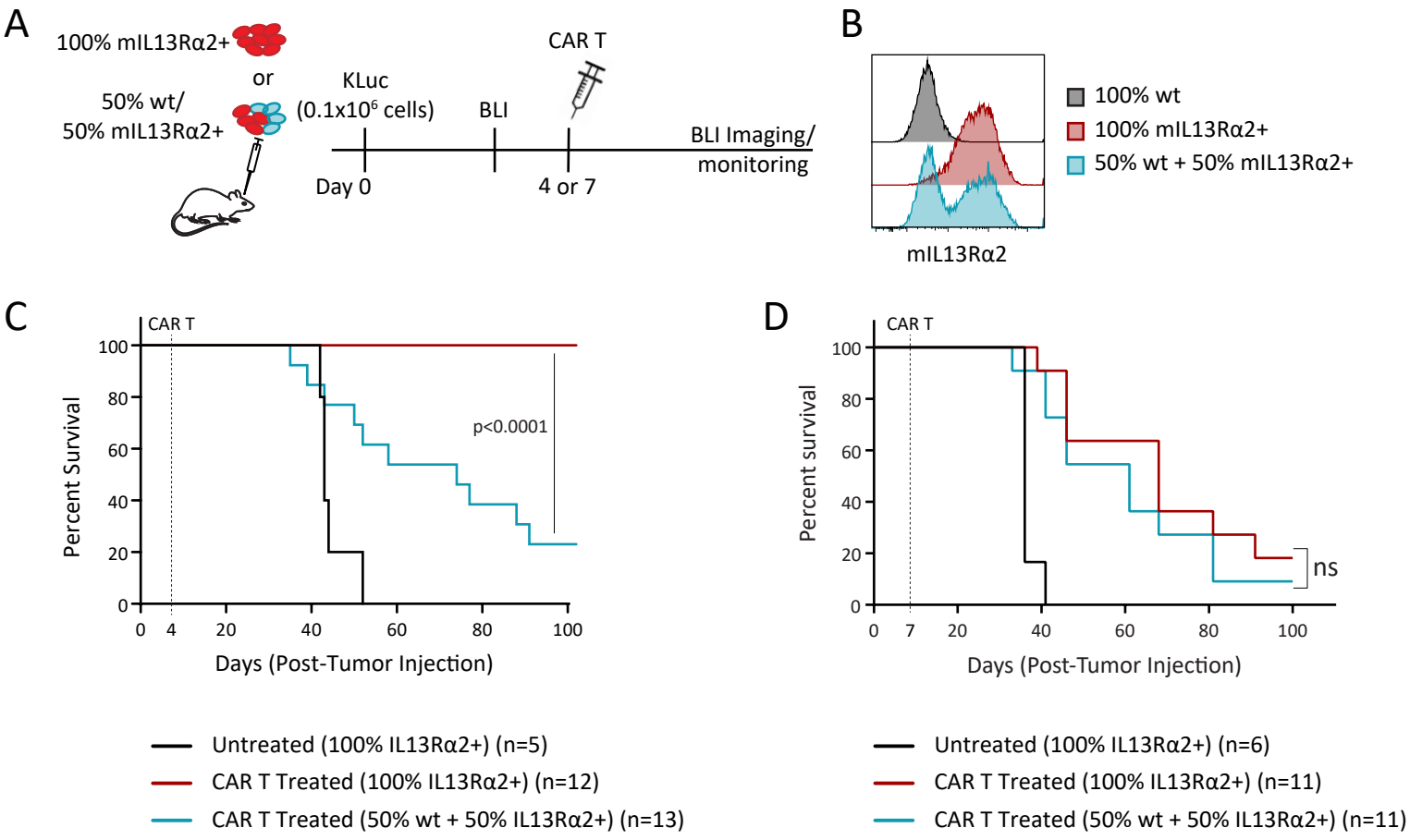

Supplementary Figure S9. Comparison of survival in mice bearing mixed antigen tumors. **A,** Schema of day 4 and 7 in vivo experimental design. **B,** Representative flow cytometry showing different levels of mIL13Rα2. **C,** Survival curve of mice bearing day 4 K-Luc-mIL13Rα2+ tumors in untreated and CAR T treated groups. **D,** Survival curve of mice bearing day 7 K-Luc-mIL13Rα 2+ tumors in untreated and CAR T treated groups. Differences between survival curves (**C** and **D**) were analyzed by log-rank (Mantel–Cox) test.

Supplementary Figure S10

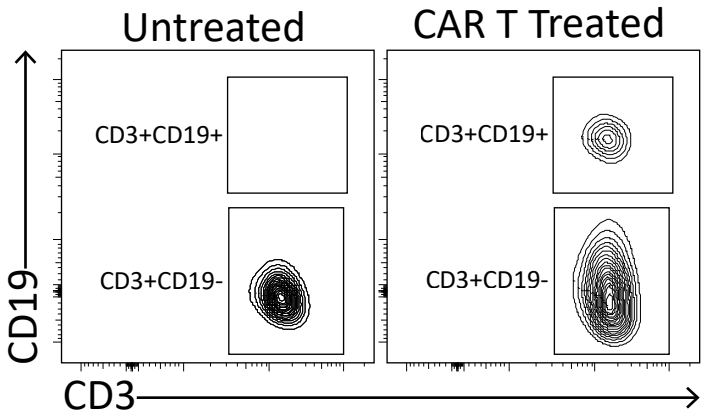

Supplementary Figure S10. Flow cytometry sort of endogenous and CAR T cells. A representation of flow cytometry sort of endogenous (CD3+CD19-) and CAR T (CD3+CD19+) populations from K-Luc-mIL13Rα2 bearing mice.

Supplementary Figure S11

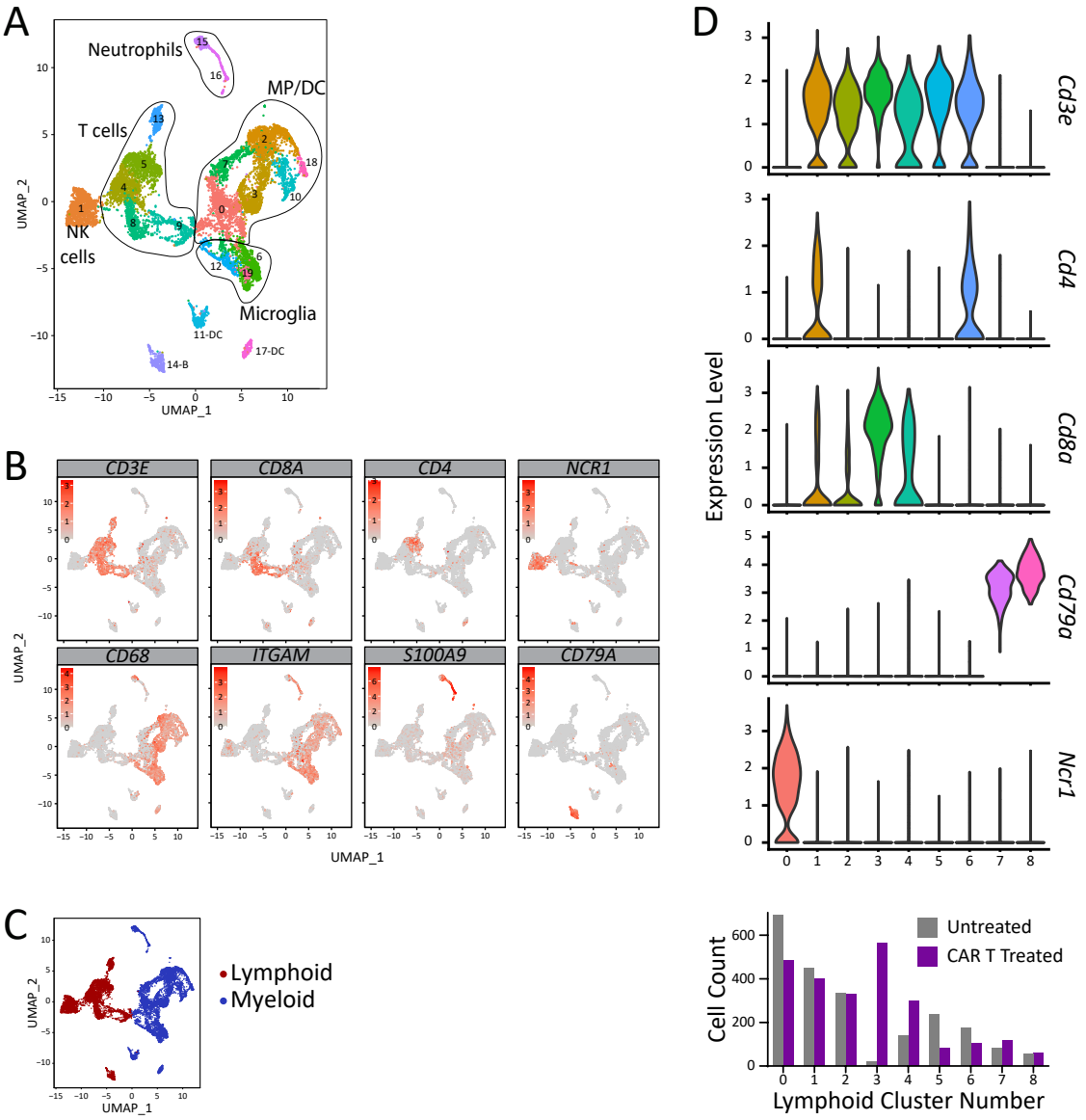

Supplementary Figure S11. Single cell RNA sequencing of intratumoral lymphoid population. A, UMAP plot from merged untreated and CAR T treated data of exclusively intratumoral immune cells. **B,** Feature plot of immune subset-specific marker-gene expression. **C,** UMAP plot shows intratumoral lymphoid and myeloid compartments. **D,** Violin plots (top) depict lymphoid specific markers and bar graph demonstrates changes in frequency of lymphoid subclusters (bottom).

Supplementary Figure S12

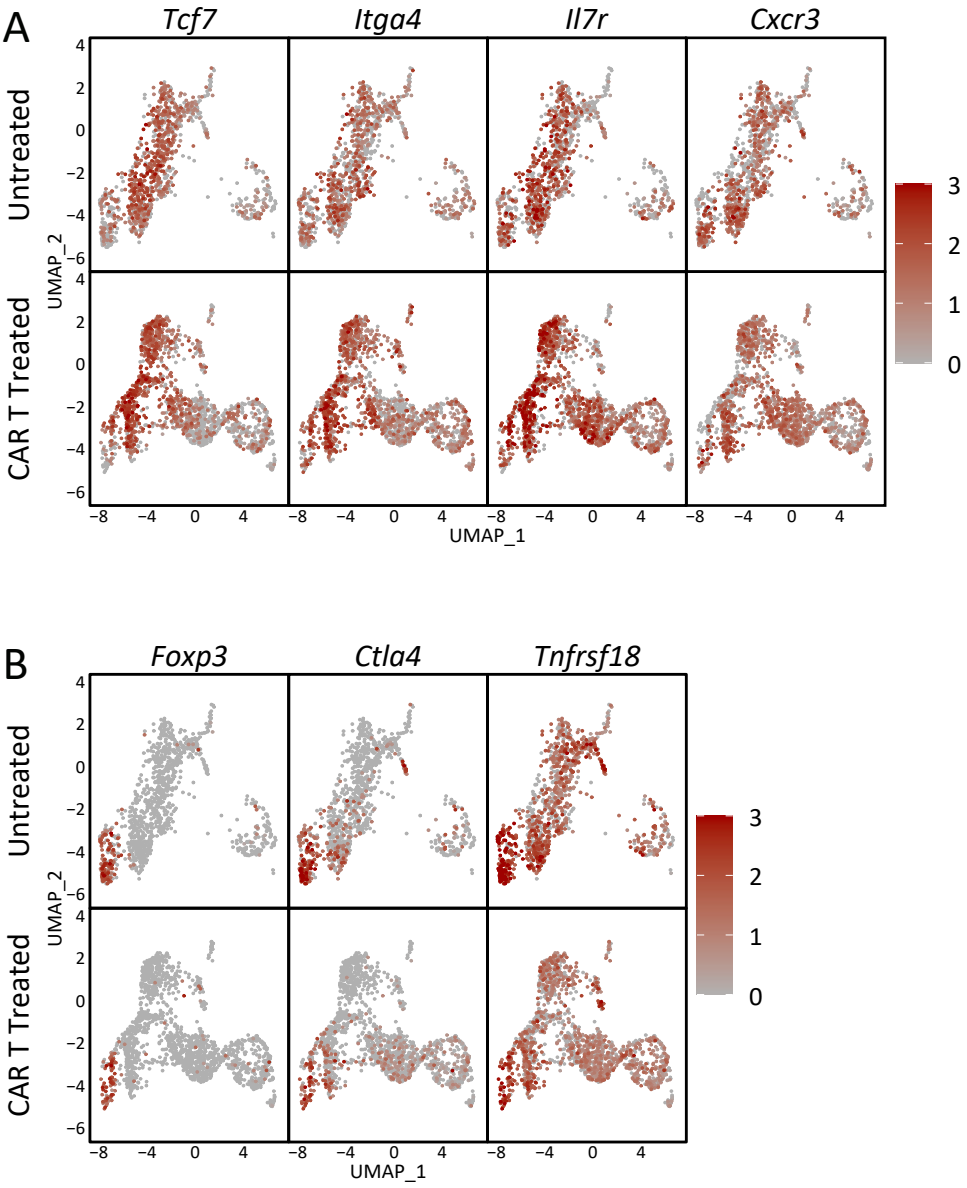

Supplementary Figure S12. Single-cell RNA sequencing identifies phenotypes of intratumoral T cells. A, UMAP plots demonstrate enhancement of genes associated with memory stem like T cells after CAR T therapy. **B,** UMAP plots demonstrate reduction in expression of genes associated with T regulatory cells after CAR T therapy.

Supplementary Figure S13

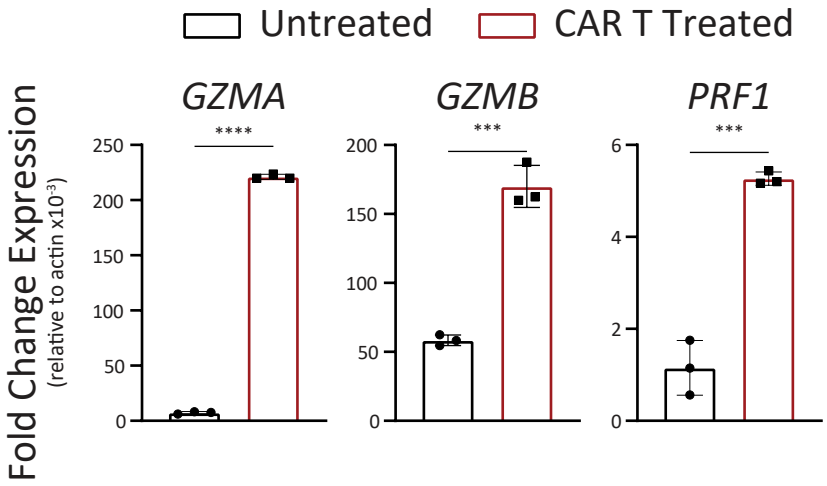

Supplementary Figure S13. Expression of genes associated with T cell activation in intratumoral T cells. qPCR analysis shows genes associated with T cell activation. Data are presented as means ± s.e.m. and were analyzed by two-tailed, unpaired Student's t-test. *p < 0.05, **p < 0.01, ***p < 0.001 and ****p < 0.0001 for indicated comparison.

Supplementary Figure S14

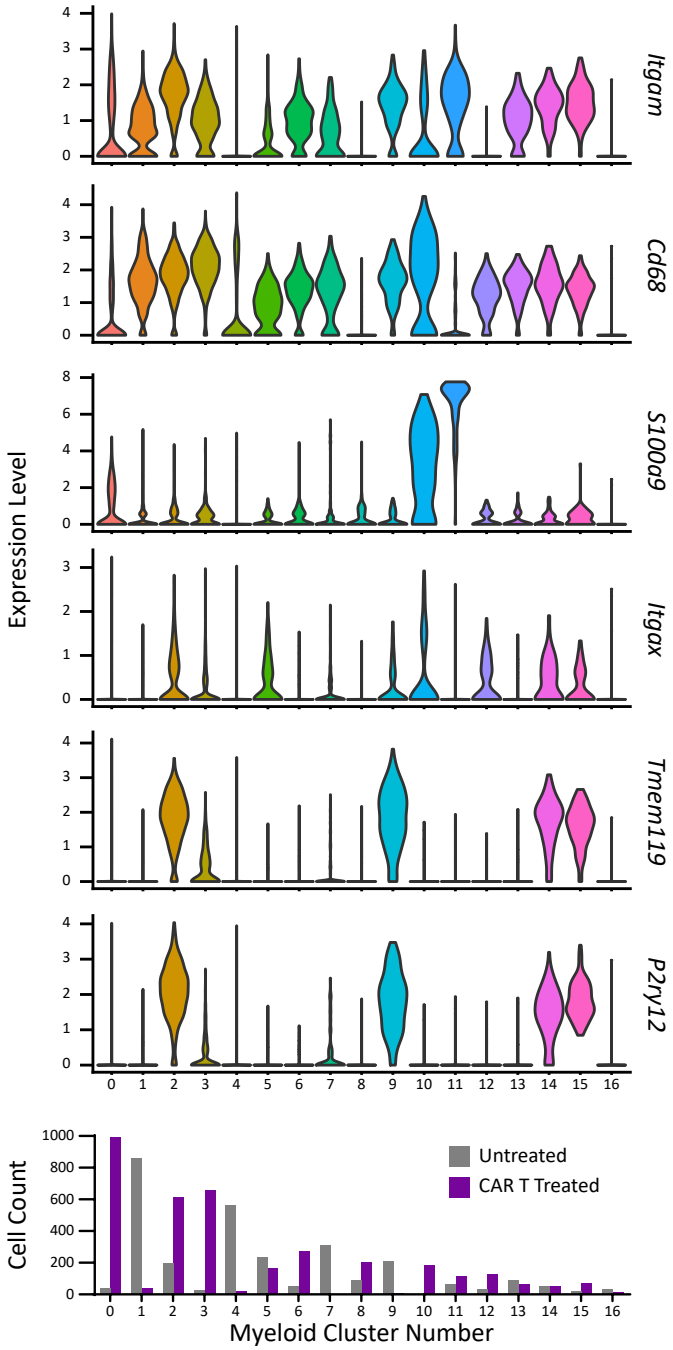

Supplementary Figure S14. Single cell RNA sequencing of intratumoral myeloid population. Violin plots (top) depict myeloid specific markers and bar graph demonstrates changes in frequency of myeloid subclusters (bottom).

Supplementary Figure S15

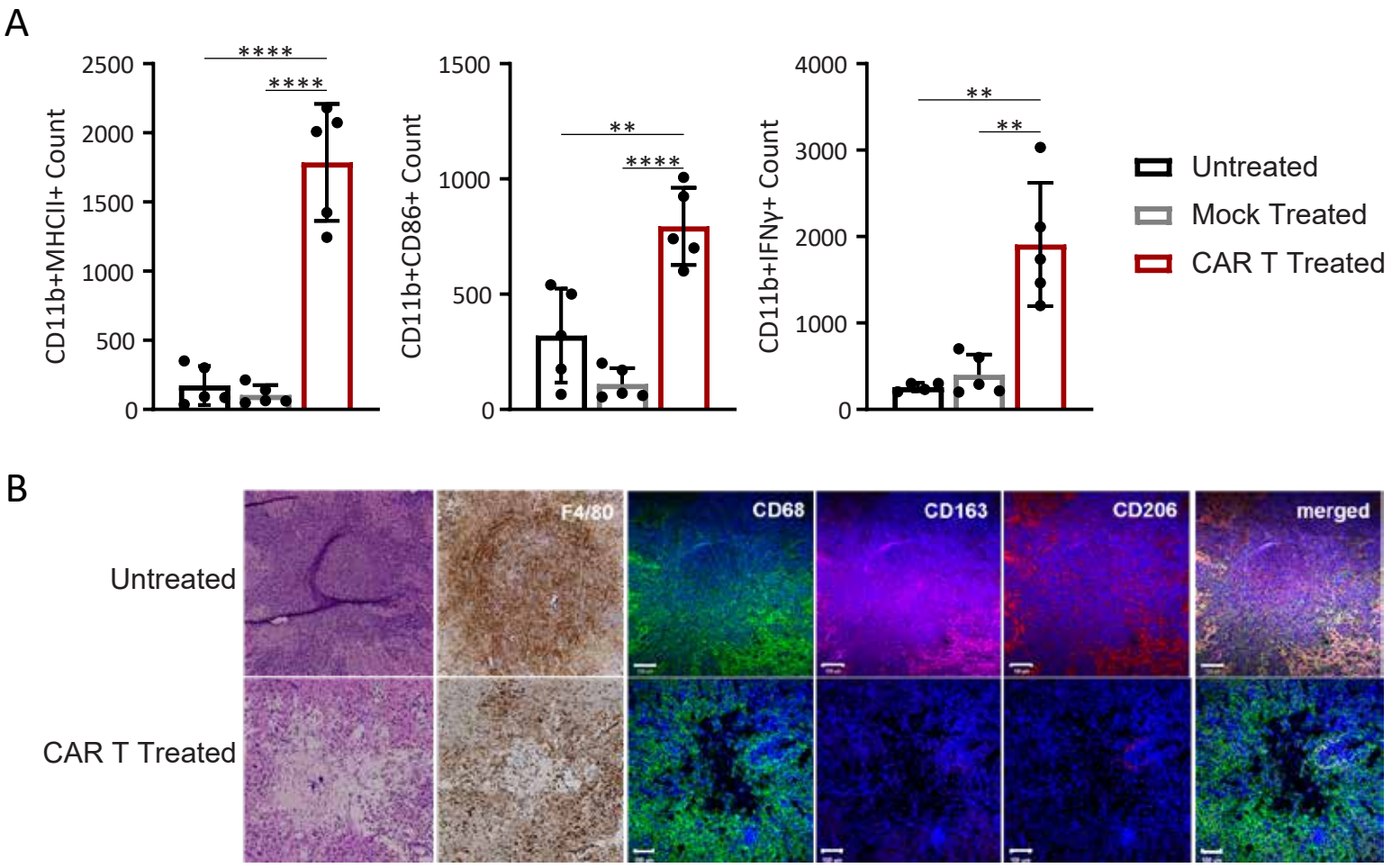

Supplementary Figure S15. Characterization of intratumoral macrophage after CAR T treatment. A, Bar graphs demonstrate number of M1 macrophages (MHCII+, CD86+ and IFNγ+) in the TME. **B,** Representative image of hematoxylin and eosin (H&E) staining shows morphology of K-Luc tumor, immunohistochemistry of F4/80 and immunofluorescent staining of CD68, CD163 and CD206 of markers on intratumoral macrophages in untreated and CAR T treated K-Luc-mIL13Rα2+ tumor bearing mice. Scale bar is 100 μm.

Supplementary Figure S16

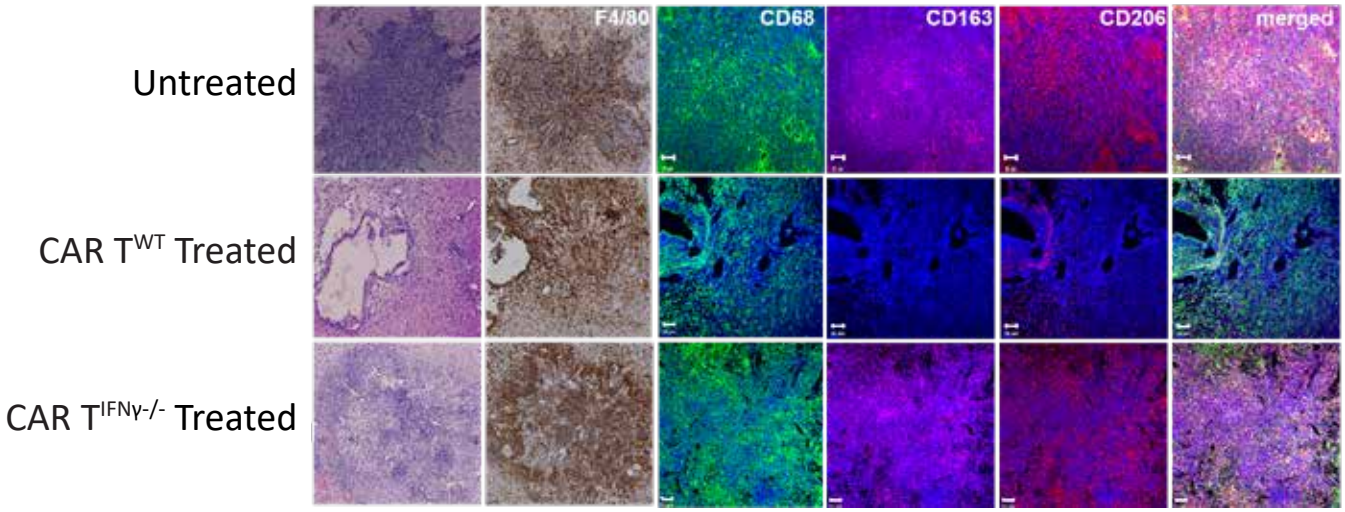

Supplementary Figure S16. Lack of IFNγ production by CAR T cells preserves the M2 type macrophages. Hematoxylin and eosin (H&E) staining demonstrates tumor site (left), immunohistochemistry of F4/80 and immunofluorescent staining of CD68, CD163 and CD206 markers on intratumoral macrophages in untreated, CAR T treated and CAR T$^{IFNγ-/-}$ treated K-Luc-mIL13Rα2+ tumor bearing mice. Scale bar is 50 μm.

Supplementary Figure S17

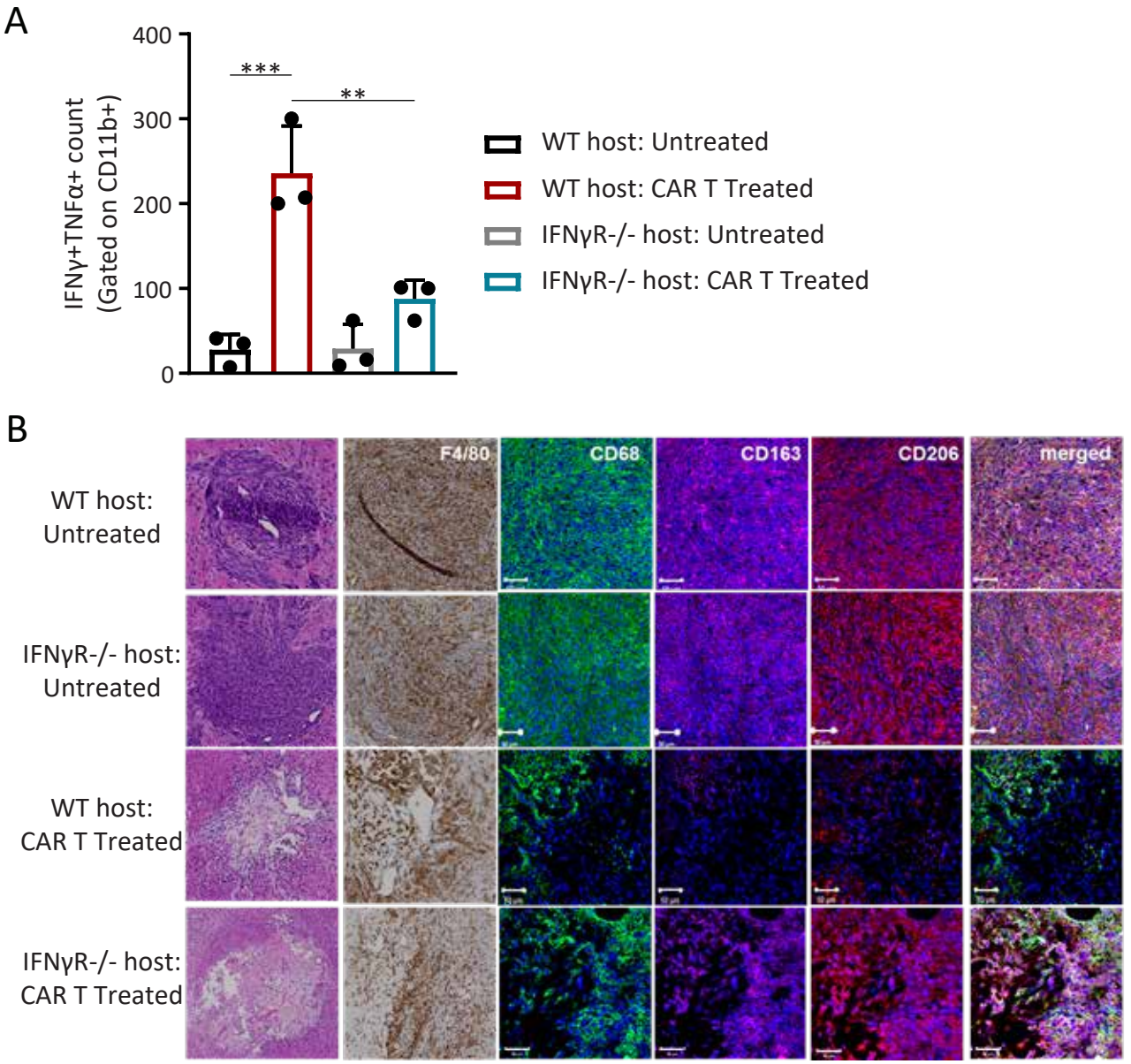

Supplementary Figure S17. Characterization of intratumoral macrophages after CAR T therapy in IFNγR-/- tumor-bearing host. A, Bar graph summarizes intratumoral IFNγ+TNFα+ macrophages (CD11b+CD45+) by flow cytometry. **B,** H&E staining demonstrates tumor site (left), immunohistochemistry of F4/80 and immunofluorescent staining of CD68, CD163 and CD206 markers on intratumoral macrophage in untreated, CAR T treated and CAR $T^{IFNγ-/-}$ treated K-Luc-mIL13Rα2+ tumor bearing mice. Scale bar is 50 μm.

Supplementary Figure S18

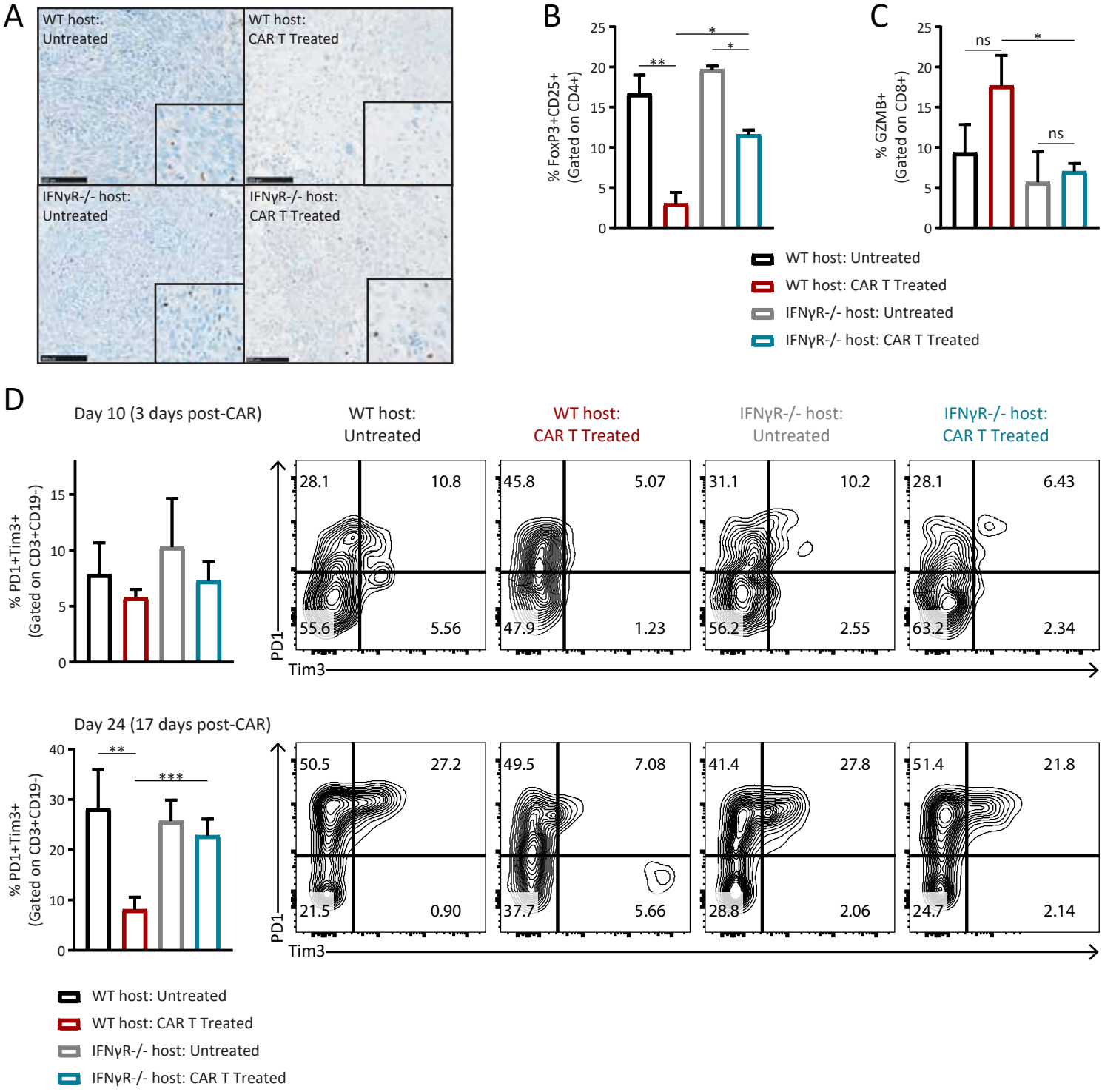

Supplementary Figure S18. Characterization of different T cell populations in WT and IFNγ R-/- host after CAR T therapy. A, Immunohistochemistry of FoxP3 marker in TME. Bar graphs show changes in frequency of **B,** regulatory T cells (CD4+CD25+FoxP3+) and **C,** effector T cells (CD8+GZMB+) in the TME by flow cytometry. **D,** Bar graph and representative flow cytometry plots of exhausted T cells at 3 day (top) and 17 day (bottom) after CAR T therapy. Data are presented as means ± s.e.m. graphs were analyzed by two-tailed, unpaired Student's t-test. *p < 0.05, **p < 0.01, ***p < 0.001 and ****p < 0.0001 for indicated comparison.

Supplementary Figure S19

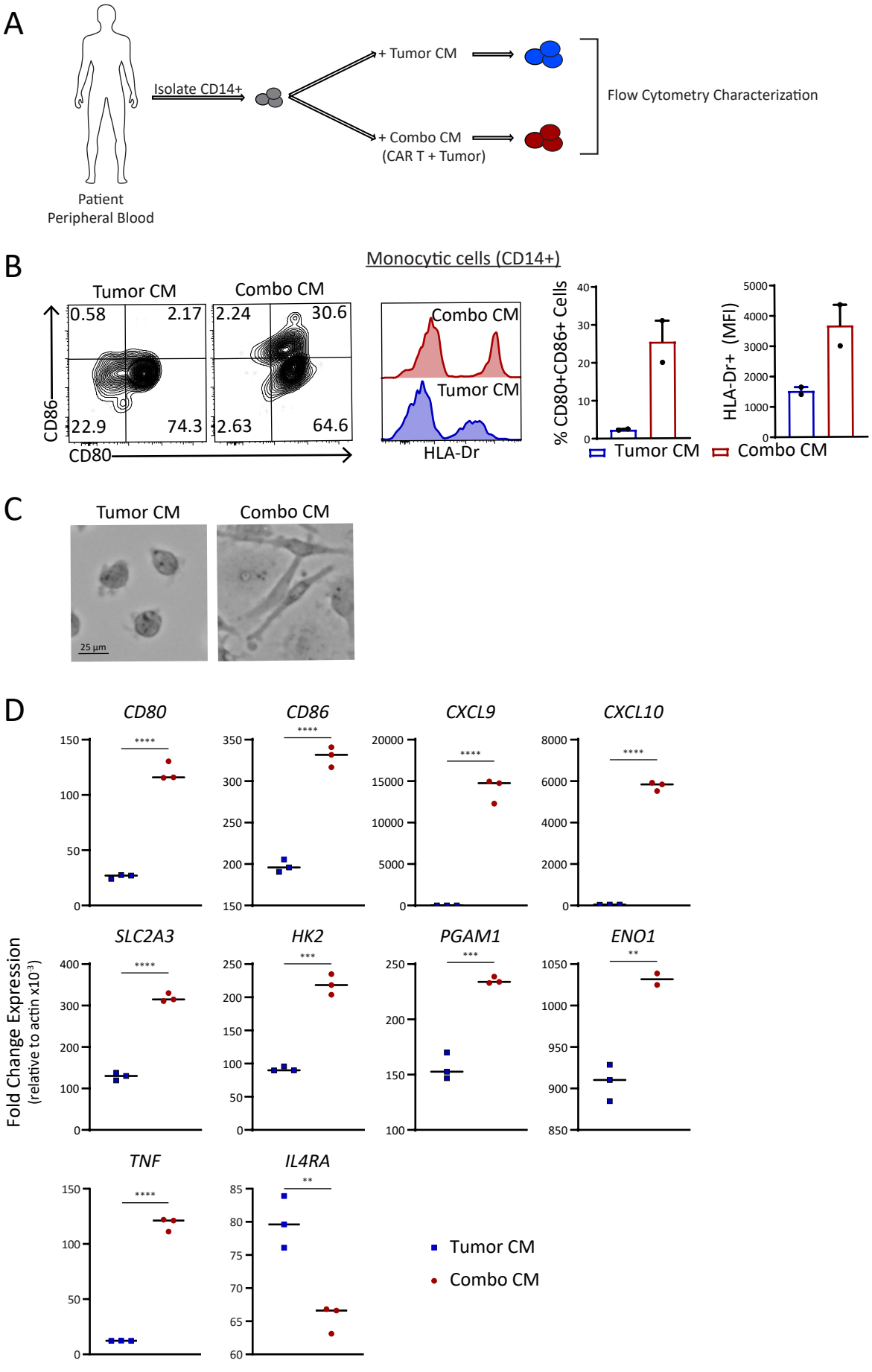

Supplementary Figure S19. CAR T cells promote monocyte differentiation and generation of M1 type macrophages. A, Schema of experimental design. **B,** Representative flow cytometry (left) and bar graphs (right) depict phenotypic changes in monocytes after incubation with conditioned media (CM) collected from tumor only (Tumor CM) or tumor-activated CAR T cells (Combo CM). **C,** Microscopy images demonstrate morphological change in monocytes after incubation with different conditioned media. **D,** qPCR analysis of genes associated with M1 macrophage phenotype. Data are presented as means ± s.e.m. and was analyzed by two-tailed, unpaired Student's t-test. *$p < 0.05$, **$p < 0.01$, ***$p < 0.001$ and ****$p < 0.0001$ for indicated comparison.